



OPEN ACCESS

EDITED BY
Yizhong Shen,
Hefei University of Technology, China

REVIEWED BY
Zhiyi Yao,
China Agricultural University, China
Xinai Zhang,
Jiangsu University, China

*CORRESPONDENCE
Hongliang Tang
tanghl2004@gxctcmu.edu.cn
Jiyang Liu
liujyxx@126.com

†These authors have contributed
equally to this work

SPECIALTY SECTION
This article was submitted to
Nutrition and Food Science
Technology,
a section of the journal
Frontiers in Nutrition

RECEIVED 06 June 2022
ACCEPTED 01 August 2022
PUBLISHED 15 August 2022

CITATION
Luo X, Zhang T, Tang H and Liu J
(2022) Novel electrochemical and
electrochemiluminescence
dual-modality sensing platform for
sensitive determination of
antimicrobial peptides based on probe
encapsulated liposome and
nanochannel array electrode.
Front. Nutr. 9:962736.
doi: 10.3389/fnut.2022.962736

COPYRIGHT
© 2022 Luo, Zhang, Tang and Liu. This
is an open-access article distributed
under the terms of the [Creative
Commons Attribution License \(CC BY\)](#).
The use, distribution or reproduction
in other forums is permitted, provided
the original author(s) and the copyright
owner(s) are credited and that the
original publication in this journal is
cited, in accordance with accepted
academic practice. No use, distribution
or reproduction is permitted which
does not comply with these terms.

Novel electrochemical and electrochemiluminescence dual-modality sensing platform for sensitive determination of antimicrobial peptides based on probe encapsulated liposome and nanochannel array electrode

Xuan Luo^{1†}, Tongtong Zhang^{2†}, Hongliang Tang^{3*} and Jiyang Liu^{1*}

¹Department of Chemistry, Key Laboratory of Surface and Interface Science of Polymer Materials of Zhejiang Province, Zhejiang Sci-Tech University, Hangzhou, China, ²Department of Hepatobiliary and Pancreatic Surgery, The Center for Integrated Oncology and Precision Medicine, Affiliated Hangzhou First People's Hospital, Zhejiang University School of Medicine, Hangzhou, China, ³Affiliated Fangchenggang Hospital, Guangxi University of Chinese Medicine, Fangchenggang, China

With the increasing application of antimicrobial peptides (AMPs) to replace antibiotics in medicine, food and agriculture, it is highly desired to develop a fast, reliable, and convenient strategy for sensitive detection of AMPs. Herein, a novel electrochemical (EC) and electrochemiluminescence (ECL) dual-modality sensing platform was developed based on probe encapsulated liposomes and nanochannel array modified electrodes, which enables sensitive determination of nisin in food samples. The bifunctional probe with both EC and ECL signals, tris(2,2-bipyridyl) dichlororuthenium (II) ($\text{Ru}(\text{bpy})_3^{2+}$), was chosen to be easily encapsulated in liposomes ($\text{Ru}(\text{bpy})_3^{2+}@liposome$). Based on the unique sterilization mechanism that AMPs can disrupt cell membranes, $\text{Ru}(\text{bpy})_3^{2+}@liposome$ can be destroyed by nisin and release a large number of $\text{Ru}(\text{bpy})_3^{2+}$ probes. Vertically-ordered mesoporous silica-nanochannel film (VMSF) modified ITO electrodes (VMSF/ITO) prepared by electrochemically assisted self-assembly (EASA) method were applied as the sensing electrode. Due to the efficient enrichment of $\text{Ru}(\text{bpy})_3^{2+}$ by the negatively charged nanochannel arrays, VMSF/ITO enables detection of the EC/ECL signals of the released $\text{Ru}(\text{bpy})_3^{2+}$ probes with ultrahigh sensitivity. In consequence, sensitive dual-modality detection of nisin was achieved by the combination of $\text{Ru}(\text{bpy})_3^{2+}@liposome$ and VMSF/ITO. The developed sensing system can realize sensitive determination of nisin in ECL mode in the concentration range of 10 ng/ml to 50 $\mu\text{g}/\text{ml}$ with a limit of detection (LOD) of 9.3 ng/ml, or in EC

mode from 800 ng/ml to 100 µg/ml with a LOD of 70 ng/ml. Combined with the excellent anti-fouling and anti-interference performance of VMSF, rapid and sensitive detection of nisin in milk or egg white was also achieved by the sensor.

KEYWORDS

electrochemical and electrochemiluminescence detection, dual-modality sensor, antimicrobial peptide, liposome, nanochannel array, food analysis

Introduction

With the long-term and widespread application of antibiotics, the resistance of pathogenic bacteria is becoming more and more serious, which poses serious hazards to food and environmental safety as well as human health. Therefore, the development of new harmless antibiotics is of great significance. The discovery of antimicrobial peptides (AMPs, also known as bactericidal peptides) provides new perspectives and broad sources for the development of new antibiotics. AMPs are small molecular polypeptides with biological activity induced in organisms. They have a wide range of antibacterial activities and also have inhibitory effects on fungi, protists, tumor cells and viruses (1). Unlike antibiotics that act on glycoproteins on the cell membrane surface (2), AMPs interact with the phospholipid bilayer of the cell membrane, killing cells or bacteria by causing rupture of the cell membrane and leakage of cellular contents (3, 4). At present, more than 2,400 AMPs have been isolated from organisms (such as insects, birds, fish, amphibians, and mammals, etc.), some of which have already been prepared on a large scale by genetic engineering (5–7). Up to now, AMPs have been widely used in medicine, food, animal husbandry and other fields (8–10). For example, nisin is a positively charged amphiphilic antimicrobial peptide containing 34 amino acid residues (11), which can effectively inhibit most Gram-positive bacteria and some Gram-positive bacteria that cause food spoilage. Since nisin is extremely sensitive to proteolytic enzymes, it can be quickly enzymatically decomposed into amino acids after consumption, and has no toxic and side effects on the human body. As a safe and efficient food preservative, nisin has replaced or partially replaced chemical preservatives in more than 60 countries and regions around the world for the preservation of dairy products, canned foods, meat products, baked goods and beverages.

The detection of AMPs is the key to their preparation and application. For example, nisin is mainly produced by microbial fermentation. The fermentation endpoint is affected by the amount and activity of bacteria, while nisin is unstable in the fermentation broth. Thus, it is necessary to adjust parameters or end the fermentation process in time to ensure the maximum yield and the minimum cost. At present, the purity of nisin produced by different companies in the market varies greatly

and even some products are far below the national standard. In addition, when nisin is used as a food additive, the concentration and activity of nisin will also decrease during food processing and storage due to the influence of temperature, pH value and composition of different foods. Accurate quantification analysis of nisin is essential for determining its level in food and assessing its stability over the shelf life of food (12, 13). Until now, the detection strategies of nisin include antibacterial detection (e.g., agar diffusion method and turbidity colorimetric), immunoassay (e.g., enzyme-linked immunosorbent assay-ELISA, immunoblotting), bioluminescence detection (e.g., aptamer-based bioluminescence assay, biosensors), and high performance liquid chromatography (HPLC) (14–19). However, these methods usually suffer from complex operations, long detection times, and high manipulation skills. Therefore, a fast, reliable, and convenient strategy for the sensitive detection of nisin is highly desired.

Electrochemistry (EC) and electrochemiluminescence (ECL) are the most widely used analytical methods due to their advantages of high sensitivity, simple operation, fast response, and potential for online monitoring (20–25). In comparison, the instrument of EC is simpler, while the sensitivity of ECL is generally higher. EC/ECL dual-modality detection can further improve the reliability and accuracy. However, nisin itself has no electroactive or ECL properties. Until now, the detection of nisin by EC or ECL methods has not been reported. Very recently, the construction of specific nanostructures on the electrode surface provides a new strategy to achieve indirect detection of non-electroactive substances (26–30). Amongst, vertically-ordered mesoporous silica-nanochannel film (VMSF) modified electrodes have attracted extensive attention. VMSF consists of a highly ordered array of nanochannels perpendicular to the electrode substrate with uniform pore size (typically 2–3 nm), ultrathin thickness (typically 50–200 nm), and high pore density (75,000/µm²) (31). This unique nanochannel array exhibits permselectivity based on material size, charge, or hydrophilicity, which makes VMSF-modified electrodes resistant to contamination and interference (32). On the one hand, the size exclusion of ultra-small pores enables VMSF to prevent particles (e.g., particles or cells) or biomacromolecules (e.g., proteins, DNA, etc.) from entering the nanochannels, improving the anti-fouling performance

of sensing electrodes. On the other hand, deionization of silanol groups ($pK_a \sim 2$) on the nanochannel surface makes VMSF negatively charged under normal pH conditions, thereby repelling negatively charged electroactive small molecules. For example, interference caused by common redox species in complex samples such as ascorbic acid (AA) or uric acid (UA) can be avoided. Furthermore, it is worth noting that VMSF nanochannels can enrich analytes through electrostatic or hydrogen bonding interactions, leading to significant signal amplification. For example, the commonly used positive ECL probe tris(2,2-bipyridyl) dichlororuthenium (II) ($\text{Ru}(\text{bpy})_3^{2+}$) can be efficiently enriched by VMSF, increasing the detection sensitivity by two orders of magnitude (33). Therefore, VMSF modified electrodes have great potential for direct and highly sensitive EC/ECL dual-modality detection of complex samples without separation or enrichment pre-treatment.

In this paper, an EC/ECL dual-modality sensing platform for the high-sensitivity determination of antimicrobial peptides was established for the first time by combining the interaction mechanism of antimicrobial peptides with cell membranes and the excellent performance of VMSF-modified electrodes such as signal amplification, anti-fouling and anti-interference. As a proof-of-concept demonstration, liposomes were used to mimic cell membranes and encapsulated a large amount of $\text{Ru}(\text{bpy})_3^{2+}$ as signal molecules for both EC and ECL detection ($\text{Ru}(\text{bpy})_3^{2+}$ @liposome). When nisin interacted with the liposomes to cause their rupture, the inner $\text{Ru}(\text{bpy})_3^{2+}$ probes were released and could be sensitively detected in an EC/ECL mode (signal-on) through the efficient enrichment of these positive probes by the VMSF nanochannel arrays. By measuring the EC or ECL signals of $\text{Ru}(\text{bpy})_3^{2+}$ on the VMSF modified electrode, a highly sensitive and signal-on dual-modality detection of nisin was obtained. Combined with the anti-interference and anti-fouling properties of VMSF, rapid and highly sensitive detection of nisin in milk or egg white was achieved.

Materials and methods

Chemicals and materials

Cetyltrimethylammonium bromide (CTAB), tetraethoxysilane (TEOS), CHCl_3 , CH_3OH , NaH_2PO_4 , Na_2HPO_4 , potassium hydrogen phthalate (KHP), potassium ferricyanide ($\text{K}_3[\text{Fe}(\text{CN})_6]$), ferrocenemethanol (FcMeOH), cysteine (L-Cys), glycine (Gly), bovine serum albumin (BSA), glucose (Glu), ascorbic acid (AA) and lactose were purchased from Aladdin Chemistry (China). Cholesterol, 1,2-dimyristoyl-sn-glycero-3-phosphocholine (DMPC), 1,2-ditetradecanoyl-sn-glycero-3-[phospho-rac-(1-glycerol)] sodium salt (DMPG), nisin, potassium ferricyanide ($\text{K}_3[\text{Fe}(\text{CN})_6]$), potassium ferrocyanide ($\text{K}_4[\text{Fe}(\text{CN})_6]$) and

potassium chloride (KCl) were obtained from Macklin (China). Hexaammineruthenium (III) chloride ($\text{Ru}(\text{NH}_3)_6\text{Cl}_3$) and Tris(2,2-bipyridine)dichlororuthenium(II) hexahydrate ($\text{Ru}(\text{bpy})_3\text{Cl}_2 \cdot 6\text{H}_2\text{O}$) were purchased from Sigma-Aldrich (USA). Milk and egg white were obtained from the local supermarket (Hangzhou, China). Ultrapure water ($18.2 \text{ M}\Omega \text{ cm}$) was used throughout the work to prepare the aqueous solutions. ITO electrodes (ITO coated glasses, $<17 \text{ }\Omega/\text{square}$, thickness: $100 \pm 20 \text{ nm}$) were obtained from Zhuhai Kaivo Optoelectronic Technology (China). Before use, The ITO electrodes were firstly cleaned using NaOH solution (1 M) and then sonicated in acetone, ethanol, and ultrapure water, respectively.

Measurements and instrumentations

Transmission electron microscopy (TEM) photographs were taken on a JEM-2100 transmission electron microscope (JEOL Co., Ltd., Japan) at a working voltage of 200 kV. Scanning electron microscopy (SEM) was performed on a field emission scanning electron microscope (S-4800, Hitachi, Japan). Ultraviolet-Vis (UV-Vis) absorption spectra were recorded on a UV-Vis spectrometer (UV-2450; Shimadzu, Japan). ECL measurements were performed using a CHI 660D electrochemical workstation (CH Instrument, China) and an MPI multifunctional ECL analyzer (Xi'an Remex Analytical Instrument Ltd., China). All electrochemical measurements were performed on an Autolab PGSTAT302N electrochemical workstation (Metrohm, Switzerland). Amongst, cyclic voltammetry (CV) scanning was performed over a potential range of 0–1.4 V at a scan rate of 100 mV/s. The DPV curves were obtained using a certain step (0.005 V), modulation amplitude (0.05 V), modulation time (0.05 s), and interval time (0.2 s). The three-electrode system was used for CV and DPV experiments. VMSF modified ITO (VMSF/ITO) was used as the working electrode, an Ag/AgCl (saturated with KCl solution) was employed as the reference electrode, and a platinum wire was applied as the counter electrode.

Preparation of VMSF modified ITO electrodes

As previously reported (34), VMSF modified ITO electrodes were rapidly fabricated by an electrochemically assisted self-assembly (EASA) method. Briefly, 20 ml NaNO_3 (0.1 M, pH = 3) and 20 ml ethanol were mixed. Then, TEOS (2.833 g) and CTAB (1.585 g) were added and the mixture was stirred for 2.5 h to obtain the precursor solution. For VMSF growth, a constant current (-0.7 mA/cm^2) was applied on an ITO electrode for 10 s. Then the electrode was quickly rinsed with ultrapure water. After being dried under N_2 , the obtained electrode was aged at

120°C for 12 h. The as-prepared electrode retained surfactant micelles that blocked the nanochannels (SM@VMSF/ITO). The inner SM was removed through immersing the electrode in a HCl-ethanol solution (0.1 M) with stirring for 5 min. The obtained electrode with open nanochannels was termed as VMSF/ITO.

Preparation of Ru(bpy)₃²⁺-encapsulated liposomes

Ru(bpy)₃²⁺-encapsulated liposomes (Ru(bpy)₃²⁺@liposome) were prepared according to the literatures with slight modifications (35, 36). Briefly, DMPG (2 mg), DMPC (8 mg) and cholesterol (8 mg) were co-dissolved in the mixture of chloroform and methanol (V/V = 1:1, 300 μl) through sonication for 5 min. After evaporation under nitrogen, the solution was put in vacuum for 4 h to remove residue organic solvent. The obtained lipid film was dissolved in PBS (1 ml, 0.01 M, pH 7.4) containing Ru(bpy)₃²⁺ (20 mM) and incubated at 30°C for 3 h. Then, the obtained mixture was sonicated in an ice water bath for 1 h to obtain a homogeneous orange suspension. The suspension was centrifuged at 15,000 rpm for 30 min to remove the free Ru(bpy)₃²⁺. The obtained precipitate was thoroughly washed using PBS (0.01 M, pH 7.4) until the supernatant was colorless. The Ru(bpy)₃²⁺@liposome was finally redispersed in 1 ml of PBS (0.01 M, pH 7.4) and stored at 4°C.

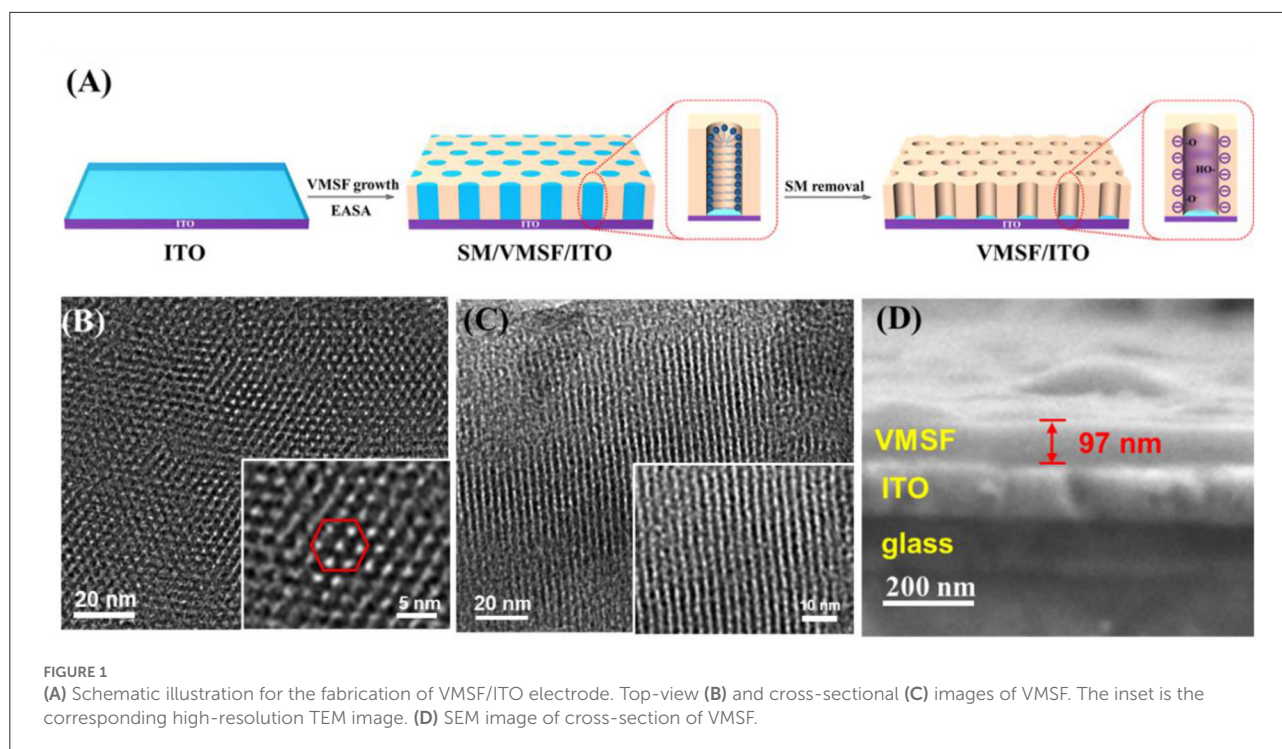
EC and ECL determination of nisin

Seven milliliter of PBS (0.01 M, pH 7.4) containing 10 μl of above Ru(bpy)₃²⁺@liposome solution or 10 μl Ru(bpy)₃²⁺@liposome and 3 mM TPrA was used as the EC or ECL detection medium. Before each measurement, different concentrations of nisin were added under slight stirring for 5 min to release Ru(bpy)₃²⁺ from liposomes. Then, the DPV or ECL signal was measured using VMSF/ITO electrode. For real sample analysis, milk and egg white were centrifuged at 10,000 rpm for 10 min to remove the interfering substances such as fat and protein (37). Due to the excellent anti-fouling and anti-interference performance of VMSF, no additional filtering step was required. Subsequently, the samples were diluted by a factor of 50 with PBS (0.01 M, pH = 7.4) and spiked with different concentrations of nisin to provide three final concentrations. Finally, nisin in milk was determined using EC method and the egg white was detected with ECL strategy.

Results and discussion

Preparation and characterizations of VMSF modified ITO electrodes

At present, the synthesis methods of VMSF mainly include Stöber solution growth method, two-phase layered growth method, electrochemical assisted self-assembly (EASA) method, etc. Due to the simple operation and fast growth (within a few



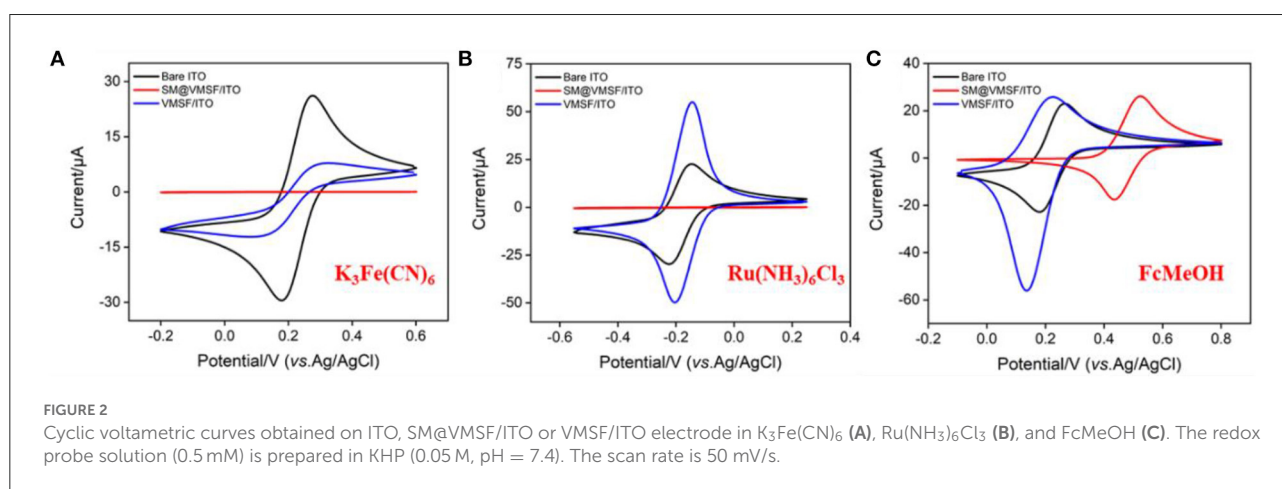
seconds), the EASA method was used to grow VMSF on the surface of ITO electrode with hexadecyl ammonium bromide micelles (CTAB) as templates (Figure 1A). When a cathodic potential was applied to the ITO electrode, the electrolysis of water resulted in a pH gradient at the electrode surface, which promoted the condensation of the silica precursor. After VMSF growth, surfactant micelles (SMs) were packed inside the nanochannels. After removing the SMs, open nanochannels were obtained and the electrode was termed as VMSF/ITO. The structure and morphology of VMSF were characterized by transmission electron microscopy (TEM) and scanning electron microscopy (SEM). The top-view TEM image of VMSF reveals a uniformly distributed nanochannel array without cracks and defects within the observed range (Figure 1B). The diameter of the nanopore is 2–3 nm (inset in Figure 1B). As displayed in the cross-sectional TEM image, nanochannels are observed to be parallel to each other and perpendicular to the electrode substrate (Figure 1C). The SEM image shows that VMSF/ITO has an obvious three-layer structure, corresponding to glass layer, ITO layer, and VMSF layer, respectively (Figure 1D). The thickness of VMSF is ~ 97 nm.

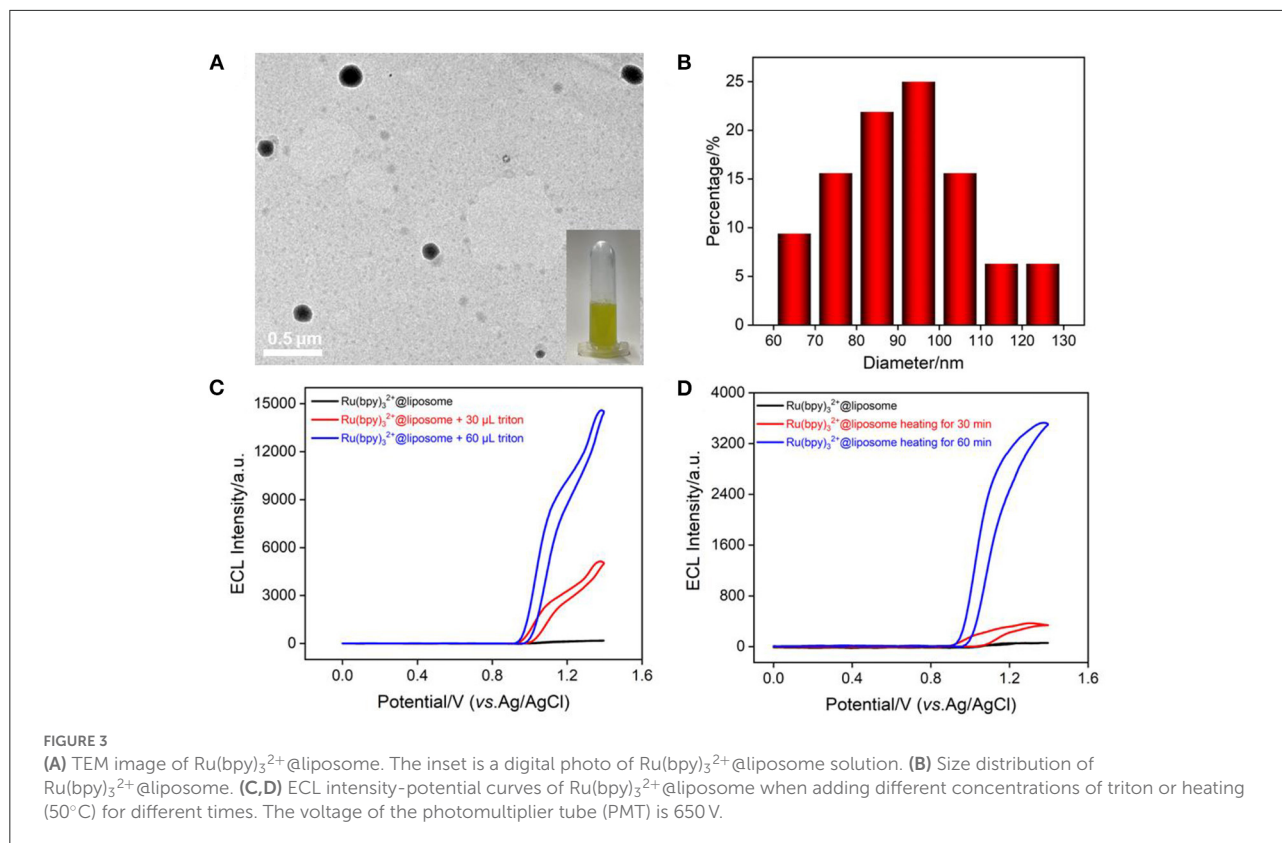
The integrity and permeability of VMSF were investigated by electrochemical characterization. CV responses of three standard electrochemical probes including an anion probe $K_3Fe(CN)_6$, a cation probe $Ru(NH_3)_6Cl_3$ and a neutral organic probe ferrocenemethanol (FcMeOH) on different electrodes were studied (Figure 2). As shown, the SM@VMSF/ITO electrode shows no signal for both $K_3Fe(CN)_6$ and $Ru(NH_3)_6Cl_3$ because the hydrophobic micelles block the nanochannels and prevent both the anionic and cationic probes from entering the pores and reaching the electrode surface. In contrast, the neutral probe FcMeOH can dissolve in micelles and reach the electrode surface through the enrichment of micelles to generate redox signals. These results prove that the VMSF completely covers the surface of the ITO electrode without defects or cracks. After SMs removal, VMSF/ITO

electrode exhibits remarkable current signals in all three probes, demonstrating the open of the nanochannel array. In comparison with bare ITO, VMSF/ITO exhibits suppressed peak current in $K_3Fe(CN)_6$ solution while enhanced signal in case of $Ru(NH_3)_6Cl_3$, demonstrating the charge-selective permeability of the nanochannels. The deprotonation of partial silanol groups ($pK_a \sim 2$) on the nanochannel surface makes the nanochannels negatively charged, thus repelling the negatively charged probes and attracting the positively charged probes. In case of FcMeOH, the reduction peak current is greater than the oxidation peak current because the oxidation products of FcMeOH are positively charged and can be enriched by the nanochannels. This remarkable charge-selective permeability is beneficial to improve the detection sensitivity of positively charged analytes, and to exclude co-existing negatively charged molecules, thereby improving the anti-interference performance of the electrode.

Characterization of $Ru(bpy)_3^{2+}$ -encapsulated liposomes

Liposome is closed vesicles with a phospholipid bilayer similar to cell membranes and can serve as a typical artificial biofilm model. In this work, liposome was used to mimic the cell membrane and the most common ECL probe with high luminescence efficiency, $Ru(bpy)_3^{2+}$, was encapsulated in liposome ($Ru(bpy)_3^{2+}@liposome$). As shown in the inset of Figure 3A, $Ru(bpy)_3^{2+}@liposome$ solution is an orange dispersion. TEM image shows that the liposome has a spherical structure (Figure 3A) with a size distribution ranging from 60 to 130 nm, with an average size of ~ 97 nm (Figure 3B). The ECL signal of $Ru(bpy)_3^{2+}$ was used to characterize its encapsulation in liposomes and the structural changes of liposomes. As shown in Figures 3C,D, the ECL signal of $Ru(bpy)_3^{2+}$ could not be detected in the solution of $Ru(bpy)_3^{2+}@liposome$,





indicating that Ru(bpy)₃²⁺ probe molecules were successfully encapsulated inside the hydrophilic cavity of liposome and thus unable to reach the electrode surface. As known, the addition of surfactants or heat can disrupt the structure of liposomes. As shown in **Figure 3C**, after the addition of surfactant triton into the Ru(bpy)₃²⁺@liposome solution, the ECL signal of Ru(bpy)₃²⁺ increased significantly with the increase of triton concentration. The ECL signal also gradually increased with the heating time. Thus, disruption of the liposome bilayer by addition of surfactant or heating results in the release of Ru(bpy)₃²⁺, thereby increasing the ECL signal.

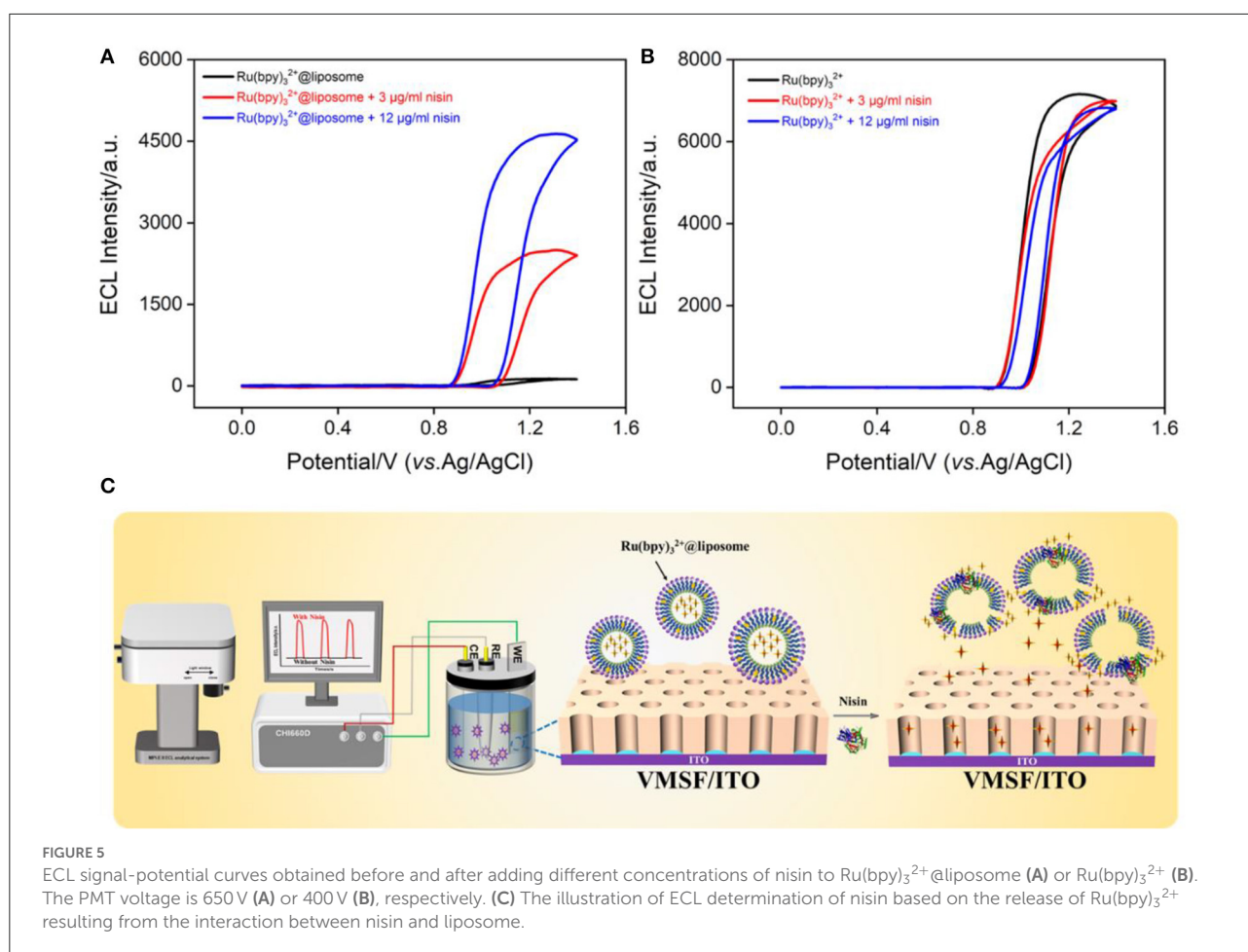
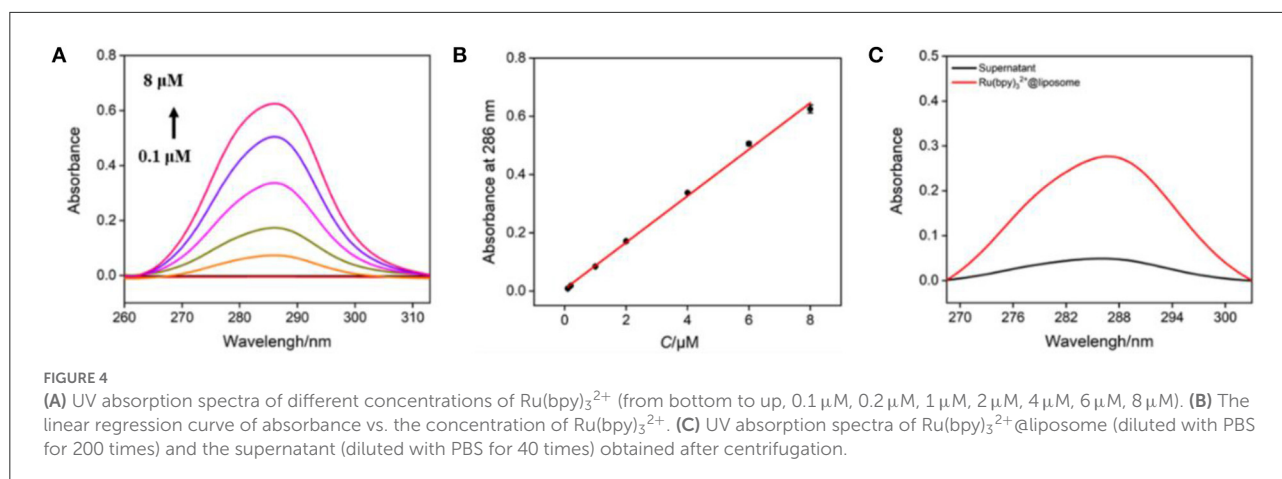
The bipyridine structure endows Ru(bpy)₃²⁺ with characteristic UV absorption (**Figure 4A**) and its absorbance (**A**) is linear with the concentration (**C**) (**Figure 4B**, $A = 0.0798 C + 0.0072$ ($R^2 = 0.997$)). As shown in **Figure 4C**, the Ru(bpy)₃²⁺@liposome solution exhibits the characteristic absorption of Ru(bpy)₃²⁺. On the contrary, there is basically no absorption in the supernatant after separation of Ru(bpy)₃²⁺@liposome through centrifugation, proving once again that Ru(bpy)₃²⁺ was encapsulated inside the hydrophilic cavity of liposomes. The amount of Ru(bpy)₃²⁺ encapsulated in liposomes was calculated to be 0.036 mg Ru(bpy)₃²⁺/mg liposome.

The electrochemical impedance spectroscopy (EIS) of Ru(bpy)₃²⁺@liposome has been investigated using ITO as the supporting electrode (**Supplementary Figure S1** in supporting

information-SI). The schematic illustration of the equivalent circuit is also displayed as inset of **Supplementary Figure S1**, which includes solution resistance (R_s), double-layer capacitance (C_{dl}), Warburg impedance (Z_w), and apparent charge transfer resistance (R_{ct}). For comparison, the EIS plot of ITO is also studied for comparison. As shown, each curve consists of a semicircle in the high frequency region representing the electron transfer process and a linear part in the low frequency region relating to the diffusion process. In addition, the equivalent diameter of the semicircle in the high frequency region is equal to R_{ct} . After ITO electrode was modified with Ru(bpy)₃²⁺@liposome, the semicircle in the EIS plot increases, indicating the increase of R_{ct} because liposome acts as an inert layer and hinders electron transfer. This phenomenon suggests the successful preparation of Ru(bpy)₃²⁺@liposome.

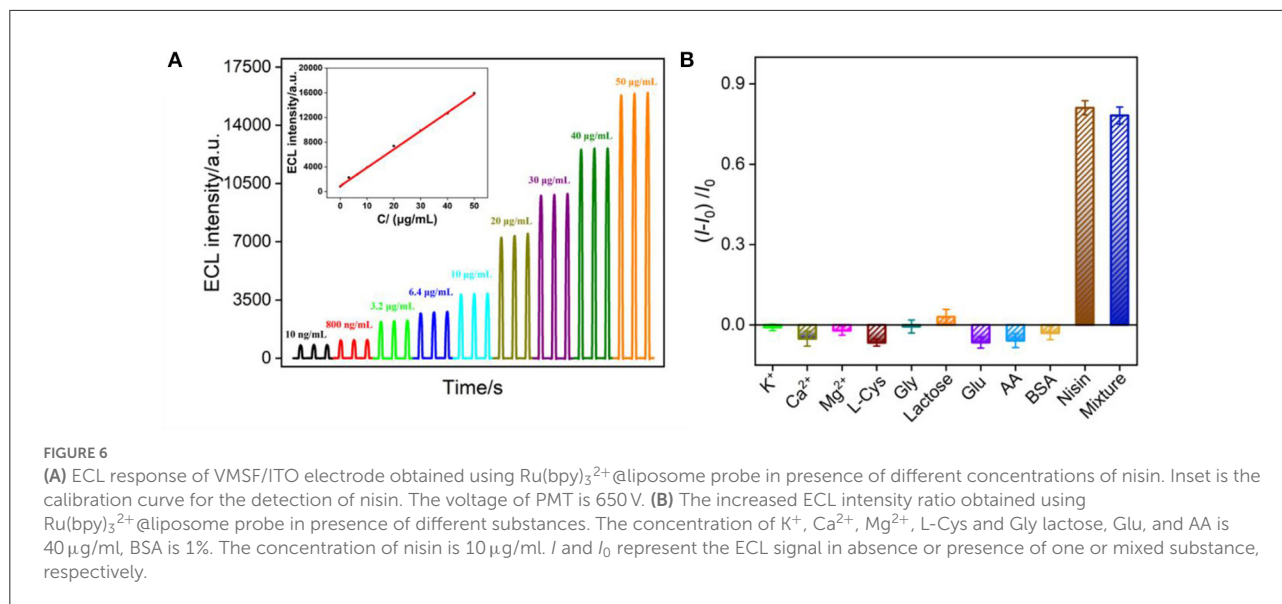
ECL of Ru(bpy)₃²⁺@liposome in presence of nisin

In comparison with other luminophore technology (e.g., fluorescence) (38–46), ECL has advantages of no background, high potential and spatial controllability, and wide response range. **Figure 5A** shows the ECL curves obtained on the



VMSF/ITO electrode in Ru(bpy)₃²⁺@liposome in the absence or presence of nisin. As seen, the ECL signal of Ru(bpy)₃²⁺ appears after the addition of nisin. And the increase of nisin concentration leads to the enhancement of the ECL signal. However, no significant change in ECL signal was observed in the control Ru(bpy)₃²⁺ solution after addition

of nisin (Figure 5B). Thus, nisin could not act as a co-reactant to promote the ECL intensity of Ru(bpy)₃²⁺. The signal enhancement in Ru(bpy)₃²⁺@liposome solution after the addition of nisin is due to the disruption of the liposome structure, resulting in the leakage of Ru(bpy)₃²⁺. When Ru(bpy)₃²⁺ (~1.2 nm) is released, it could be enriched by the



negatively charged nanochannel array (2–3 nm in diameter) because of the electrostatic interaction between VMSF and Ru(bpy)₃²⁺ (47–51). Thus, the released Ru(bpy)₃²⁺ could get to the ITO surface, leading to significant ECL signal.

As known, nisin itself does not have electrochemical or electrochemiluminescence properties, so in this work, Ru(bpy)₃²⁺@liposome was synthesized and applied as a sensing membrane and probe for the detection of nisin. As shown in Figure 5C, when nisin was added, liposomes were disrupted and the released Ru(bpy)₃²⁺ could act as the source of the ECL signal. The mechanism by which nisin destroys liposomes could be attributed to two aspects. On the one hand, the positively charged C-terminus of nisin binds to the negatively charged liposomes through electrostatic interaction, resulting in a local disturbance of the phospholipid group in the head, which further forms a wedge shape channel. On the other hand, the N-terminus of nisin is rich in hydrophilic amino acid residues, while the C-terminus is rich in hydrophobic amino acid residues. When the hydrophilic group interacts with the phospholipid head group, the hydrophobic side chain is immersed in the hydrophobic core of the liposome to form pores (4). Thus, the presence of nisin can disrupt the liposomes, allowing the probe Ru(bpy)₃²⁺ to leak from the inner hydrophobic cavity. The negatively charged nanochannels on VMSF/ITO electrode can efficiently enrich Ru(bpy)₃²⁺ through electrostatic interactions, resulting in sensitive ECL signals.

ECL determination of nisin using VMSF/ITO electrode

The ECL detection of nisin using VMSF/ITO electrode was investigated based on the mechanism that nisin could destroy

the liposome structure, resulting in the release of Ru(bpy)₃²⁺ to generate ECL signals. Figure 6A shows the ECL curves obtained in Ru(bpy)₃²⁺@liposome solution with different concentrations of nisin. It can be found that the ECL signal of the solution increased with the increase of nisin concentration. When the nisin concentration ranged from 10 ng/ml to 50 µg/ml, the ECL intensity (*I*) had a good linear fitting relationship with the concentration of nisin (*C*_{nisin}) ($I = 297.5 C_{\text{nisin}} + 896.2$, $R^2 = 0.998$, inset in Figure 6A). The limit of detection (LOD) based on a three signal-to-noise ratio ($S/N = 3$) is 9.3 ng/ml.

Detection selectivity is important for the application of the developed sensor. The selectivity of VMSF/ITO electrode to detect nisin was investigated by evaluating the effects of common ions (K⁺, Ca²⁺ and Mg²⁺), some amino acids (L-cysteine, L-Cys; glycine, Gly), sugars (lactose, glucose-Glu), redox small molecules (ascorbic acid-AA), protein (bovine serum albumin-BSA), or their mixture on the detection of nisin. As shown in Figure 6B, when the concentration of the interfering substance was much higher than that of nisin, the change ratio of ECL signal calculated using ECL intensity before (*I*₀) and after (*I*) adding a single of interfering substance was significantly low, proving that the electrode had good selectivity.

EC determination of nisin using VMSF/ITO electrode

ECL generally has higher sensitivity, while EC detection requires simpler instrumentation. Though Ru(bpy)₃²⁺ can be used as an ECL probe with excellent properties, its redox properties also make it an EC probe. Therefore, the EC

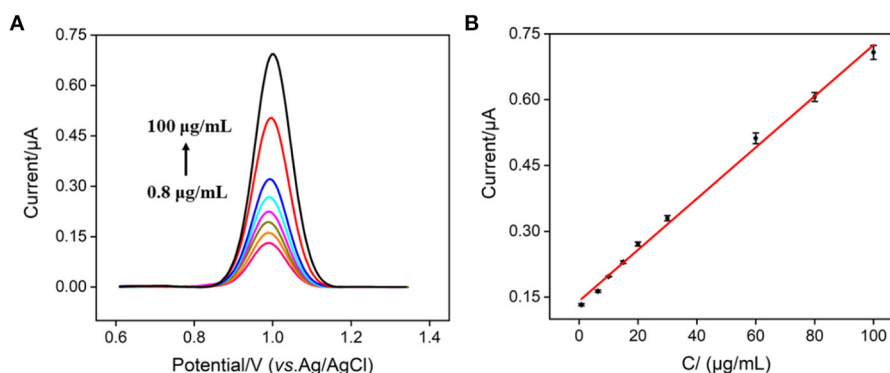


FIGURE 7
(A) DPV curves obtained on VMSF/ITO electrode in $\text{Ru}(\text{bpy})_3^{2+}$ @liposome probe containing different concentrations of nisin. **(B)** The calibration curve for the detection of nisin. The error bar represents the standard deviation of three measurements.

detection of nisin can be simultaneously realized by measuring the electrochemical signal of $\text{Ru}(\text{bpy})_3^{2+}$. Figure 7A shows the DPV curves obtained in $\text{Ru}(\text{bpy})_3^{2+}$ @liposome solution in the presence of different concentrations of nisin. The oxidation peak current of $\text{Ru}(\text{bpy})_3^{2+}$ increased with the increase of the concentration of nisin. When the concentration of nisin was between 800 ng/ml and 100 μg/ml, the oxidation peak current (I) had a good linear relationship with the concentration of nisin (C_{nisin}) ($I = 0.0059 C_{\text{nisin}} + 0.1411$, $R^2 = 0.996$, Figure 7B). The LOD is 70 ng/ml ($S/N = 3$). Thus, the EC/ECL dual-modality sensing platform for the highly sensitive determination of nisin is established for the first time. Comparison between determination of nisin using different strategies is demonstrated in Supplementary Table S1 (SI) (14, 17, 52–54). The LOD obtained by EC detection is lower than that obtained from micellar electrokinetic chromatography (MEKC) (54), liquid chromatography-mass spectrophotometry/mass spectrophotometry (LC-MS/MS) (52), or capillary zone electrophoresis (CE) (53). The LOD obtained by ECL detection is the lowest amongst the above method and is also lower than that obtained from CE-contactless conductivity detection (CE-CD) (14) or LC-MS/MS (17).

Real sample analysis

To verify the performance of the sensor in real sample analysis, nisin in egg white or milk was detected using ECL or EC mode. As shown in Supplementary Table S2 (SI), the satisfactory recoveries (94.3–107.3%) and small RSD values (<3.5%) were obtained, indicating good reliability in both ECL or EC detection. This is attributed to the excellent anti-fouling and anti-interference properties of the sensing electrode provided by VMSF nanochannels.

Conclusions

In summary, we have developed the electrochemical and electrochemiluminescence dual-modality detection of antimicrobial peptides for the first time by combining the interaction mechanism between antimicrobial peptides and cells and the signal amplification effect of VMSF nanochannel arrays. $\text{Ru}(\text{bpy})_3^{2+}$ @liposome was easily synthesized and used as both sensing membrane and signal probe. Based on the efficient enrichment of $\text{Ru}(\text{bpy})_3^{2+}$ by VMSF nanochannels, the VMSF/ITO electrode can sensitively detect $\text{Ru}(\text{bpy})_3^{2+}$ probes leaked from nisin-disrupted liposomes in ECL or EC mode, thereby achieving sensitive dual-modality detection of nisin. Combined with the excellent anti-fouling and anti-interference abilities of VMSF, VMSF/ITO electrode can be used for the rapid detection of nisin in milk or egg white sample. The combination of VMSF/ITO sensing electrode and $\text{Ru}(\text{bpy})_3^{2+}$ @liposome with integrated sensitive membrane and signal probe provides a new strategy for the detection of non-electroactive antimicrobial peptides. In addition, the high detection sensitivity of ECL and the advantage that EC detection is not affected by the color or transparency of the sample make the constructed dual-modality sensing have an extended sample range.

Data availability statement

The original contributions presented in the study are included in the article/Supplementary material, further inquiries can be directed to the corresponding author.

Author contributions

XL: data curation. TZ: data curation and writing—original draft preparation. HT: writing—review and editing.

JL: supervision and writing—review and editing. All authors contributed to the article and approved the submitted version.

Acknowledgments

We acknowledge the financial support from the National Natural Science Foundation of China (21904117, 82074574, and 81774445) and the Zhejiang Provincial Natural Science Foundation of China (LY20B050007).

Conflict of interest

The authors declare that the research was conducted in the absence of any commercial or financial relationships that could be construed as a potential conflict of interest.

References

- Zasloff M. Antimicrobial peptides of multicellular organisms. *Nature*. (2002) 415:389–95. doi: 10.1038/415389a
- Keenan T, Dowle A, Bates R, Smith MCM. Characterization of the streptomyces coelicolor glycoproteome reveals glycoproteins important for cell wall biogenesis. *MBio*. (2019) 10:e01092–19. doi: 10.1128/mBio.01092-19
- Driessen A, Hooven H, Kuiper W, Kamp M, Sahl HG, Konings R. Mechanistic studies of lantibiotic-induced permeabilization of phospholipid vesicles. *Biochemistry*. (1995) 34:1606–14. doi: 10.1021/bi00005a017
- Wiedemann I, Breukink E, Van Kraaij C, Kuipers OP, Bierbaum G, de Kruijff B, et al. Specific binding of nisin to the peptidoglycan precursor lipid ii combines pore formation and inhibition of cell wall biosynthesis for potent antibiotic activity. *J Biol Chem*. (2001) 276:1772–9. doi: 10.1074/jbc.M006770200
- Czihal P, Knappe D, Fritsche S, Zahn M, Berthold N, Piantavigna S, et al. Api88 is a novel antibacterial designer peptide to treat systemic infections with multidrug-resistant gram-negative pathogens. *ACS Chem Biol*. (2012) 7:1281–91. doi: 10.1021/cb300063v
- Jenkins RJ, Dotson GD. Dual targeting antibacterial peptide inhibitor of early lipid a biosynthesis. *ACS Chem Biol*. (2012) 7:1170–7. doi: 10.1021/cb300094a
- Russell AL, Spuches AM, Williams BC, Venugopal D, Klapper D, Srouji AH, et al. The effect of the placement and total charge of the basic amino acid clusters on antibacterial organism selectivity and potency. *Bioorg Med Chem*. (2011) 19:7008–22. doi: 10.1016/j.bmc.2011.10.033
- Chen Y, Wu J, Cheng H, Dai Y, Wang Y, Yang H, et al. Anti-infective effects of a fish-derived antimicrobial peptide against drug-resistant bacteria and its synergistic effects with antibiotic. *Front Microbiol*. (2020) 11:602412. doi: 10.3389/fmicb.2020.602412
- Ghosh SK, Weinberg A. Ramping up antimicrobial peptides against severe acute respiratory syndrome coronavirus-2. *Front Mol Biosci*. (2021) 8:620806. doi: 10.3389/fmolb.2021.620806
- Wu Y, He Y, Ge X. Functional characterization of the recombinant antimicrobial peptide trx-ace-amp1 and its application on the control of tomato early blight disease. *Appl Microbiol Biotechnol*. (2011) 90:1303–10. doi: 10.1007/s00253-011-3166-x
- Harrys R, Oscarp K, Paula B. Improvement of solubility and stability of the antimicrobial peptide nisin by protein engineering. *Appl Environ Microbiol*. (1995) 61:2873–8. doi: 10.1128/aem.61.8.2873-2878.1995
- Landete JM, Langa S, Escudero C, Peiroten A, Arques JL. Fluorescent detection of nisin by genetically modified lactococcus lactis strains in milk and a colonic model: application of whole-cell nisin biosensors. *J Biosci Bioeng*. (2020) 129:435–40. doi: 10.1016/j.jbiosc.2019.10.011
- Malvano F, Pilloton R, Albanese D. A novel impedimetric biosensor based on the antimicrobial activity of the peptide nisin for the detection of salmonella spp. *Food Chem*. (2020) 325:126868–74. doi: 10.1016/j.foodchem.2020.126868
- Drevinskas T, Stankevicius M, Bimbiraite-Surviliene K, Naujokaityte G, Kaskoniene V, Kondrotiene K, et al. Optimization of a capillary zone electrophoresis-contactless conductivity detection method for the determination of nisin. *Electrophoresis*. (2018) 39:2425–30. doi: 10.1002/elps.201800143
- Hakovirta J, Reunanen J, Saris PE. Bioassay for nisin in milk, processed cheese, salad dressings, canned tomatoes, and liquid egg products. *Appl Environ Microbiol*. (2006) 72:1001–5. doi: 10.1128/AEM.72.2.1001-1005.2006
- Leung P, Khadre M, Shellhammer T. Immunoassay method for quantitative determination of nisin in solution and on polymeric films. *Lett Appl Microbiol*. (2002) 34:199–204. doi: 10.1046/j.1472-765x.2002.01072.x
- Martinez-Rios V, Pedersen M, Pedrazzi M, Gkogka E, Smedsgaard J, Dalgaard P. Antimicrobial effect of nisin in processed cheese - quantification of residual nisin by LC-MS/MS and development of new growth and growth boundary model for listeria monocytogenes. *Int J Food Microbiol*. (2021) 338:108952–62. doi: 10.1016/j.ijfoodmicro.2020.108952
- Reunanen J, Saris PE. Microplate bioassay for nisin in foods, based on nisin-induced green fluorescent protein fluorescence. *Appl Environ Microbiol*. (2003) 69:4214–8. doi: 10.1128/AEM.69.7.4214-4218.2003
- Tramer J, Fowler G. Tramer - estimation of nisin in foods. *J Sci Fd Agric*. (1964) 15:522–8. doi: 10.1002/jfsa.2740150802
- Kimmel DW, LeBlanc G, Meschievitz ME, Cliffel DE. Electrochemical sensors and biosensors. *Anal Chem*. (2012) 84:685–707. doi: 10.1021/ac202878q
- Liu Q, Zhong H, Chen M, Zhao C, Liu Y, Xi F, et al. Functional nanostructure-loaded three-dimensional graphene foam as a non-enzymatic electrochemical sensor for reagentless glucose detection. *RSC Adv*. (2020) 10:33739–46. doi: 10.1039/D0RA05553K
- Wang W, Liu Y, Shi T, Sun J, Mo F, Liu X. Biosynthesized quantum dot for facile and ultrasensitive electrochemical and electrochemiluminescence immunoassay. *Anal Chem*. (2020) 92:1598–604. doi: 10.1021/acs.analchem.9b04919
- Wei X, Luo X, Xu S, Xi F, Zhao T. A flexible electrochemiluminescence sensor equipped with vertically ordered mesoporous silica nanochannel film for sensitive detection of clindamycin. *Front Chem*. (2022) 10:872582. doi: 10.3389/fchem.2022.872582
- He L, Huang R, Xiao P, Liu Y, Jin L, Liu H, et al. Current signal amplification strategies in aptamer-based electrochemical biosensor: a review. *Chin Chem Lett*. (2021) 32:1593–602. doi: 10.1016/j.ccl.2020.12.054

Publisher's note

All claims expressed in this article are solely those of the authors and do not necessarily represent those of their affiliated organizations, or those of the publisher, the editors and the reviewers. Any product that may be evaluated in this article, or claim that may be made by its manufacturer, is not guaranteed or endorsed by the publisher.

Supplementary material

The Supplementary Material for this article can be found online at: <https://www.frontiersin.org/articles/10.3389/fnut.2022.962736/full#supplementary-material>

25. Nasir T, Herzog G, Hébrant M, Despas C, Liu L, Walcarius A. Mesoporous silica thin films for improved electrochemical detection of paraquat. *ACS Sens.* (2018) 3:484–93. doi: 10.1021/acssensors.7b00920
26. Carrara S, Arcudi F, Prato M, De Cola L. Amine-rich nitrogen-doped carbon nanodots as a platform for self-enhancing electrochemiluminescence. *Angew Chem Int Ed Engl.* (2017) 56:4757–61. doi: 10.1002/anie.201611879
27. Liang W, Zhuo Y, Xiong C, Zheng Y, Chai Y, Yuan R. Ultrasensitive cytosensor based on self-enhanced electrochemiluminescent ruthenium-silica composite nanoparticles for efficient drug screening with cell apoptosis monitoring. *Anal Chem.* (2015) 87:12363–71. doi: 10.1021/acs.analchem.5b03822
28. Gong J, Zhang T, Luo T, Luo X, Yan F, Tang W, et al. Bipolar silica nanochannel array confined electrochemiluminescence for ultrasensitive detection of SARS-CoV-2 antibody. *Biosens. Bioelectron.* (2022) 215:114563. doi: 10.1016/j.bios.2022.114563
29. Wang H, Chai Y, Li H, Yuan R. Sensitive electrochemiluminescent immunosensor for diabetic nephropathy analysis based on tris(bipyridine) ruthenium(II) derivative with binary intramolecular self-catalyzed property. *Biosens Bioelectron.* (2018) 100:35–40. doi: 10.1016/j.bios.2017.08.054
30. Zhang M, Zou Y, Zhou X, Yan F, Ding Z. Vertically-ordered mesoporous silica films for electrochemical detection of Hg(II) ion in pharmaceuticals and soil samples. *Front Chem.* (2022) 10:952936. doi: 10.3389/fchem.2022.952936
31. Zhu X, Xuan L, Gong J, Liu J, Wang X, Xi F, et al. Three-dimensional macroscopic graphene supported vertically-ordered mesoporous silica-nanochannel film for direct and ultrasensitive detection of uric acid in serum. *Talanta.* (2022) 238:123027. doi: 10.1016/j.talanta.2021.123027
32. Zou Y, Zhou X, Xie L, Tang H, Yan F. Vertically-ordered mesoporous silica films grown on boron nitride-graphene composite modified electrodes for rapid and sensitive detection of carbendazim in real samples. *Front Chem.* (2022) 10:939510. doi: 10.3389/fchem.2022.939510
33. Zhou Z, Guo W, Xu L, Yang Q, Su B. Two orders-of-magnitude enhancement in the electrochemiluminescence of Ru(bpy)₃[³⁺] by vertically ordered silica mesochannels. *Anal Chim Acta.* (2015) 886:48–55. doi: 10.1016/j.aca.2015.06.005
34. Walcarius A, Sibottiere E, Etienne M, Ghanbaja J. Electrochemically assisted self-assembly of mesoporous silica thin films. *Nat Mater.* (2007) 6:602–8. doi: 10.1038/nmat1951
35. Li Z, Tang Y, Zhang L, Wu J. Label-free study of the function of ion channel protein on a microfluidic optical sensor integrated with artificial cell membrane. *Lab Chip.* (2014) 14:333–41. doi: 10.1039/C3LC50937K
36. Liu G, Ling J, Li J. Extremely sensitive molecularly imprinted ECL sensor with multiple probes released from liposomes immobilized by a light-triggered click reaction. *ACS Sens.* (2021) 6:4185–92. doi: 10.1021/acssensors.1c01763
37. Peng H, Hui Y, Zhang L, Zhang F, Liu Y, Zheng J, et al. A novel electrochemical aptasensor based on Ti[³⁺]C[²⁺]-MOFs nanocomposites for rapid streptomycin detection in milk samples. *Sens Actuators, B.* (2022) 368:132119–28. doi: 10.1016/j.snb.2022.132119
38. Liu X, Chen Z, Wang T, Jiang X, Qu X, Duan W, et al. Tissue imprinting on 2D nanoflakes-capped silicon nanowires for lipidomic mass spectrometry imaging and cancer diagnosis. *ACS Nano.* (2022) 16:6916–28. doi: 10.1021/acsnano.2c02616
39. Duan W, Jin Y, Cui Y, Xi F, Liu X, Wo F, et al. A co-delivery platform for synergistic promotion of angiogenesis based on biodegradable, therapeutic and self-reporting luminescent porous silicon microparticles. *Biomaterials.* (2021) 272:120772–84. doi: 10.1016/j.biomaterials.2021.120772
40. Cui Y, Duan W, Jin Y, Wo F, Xi F, Wu J. Graphene quantum dot-decorated luminescent porous silicon dressing for theranostics of diabetic wounds. *Acta Biomater.* (2021) 131:544–54. doi: 10.1016/j.actbio.2021.07.018
41. Zhao J, Zheng Y, Pang Y, Chen J, Zhang Z, Xi F, et al. Graphene quantum dots as full-color and stimulus responsive fluorescence ink for information encryption. *J Colloid Interface Sci.* (2020) 579:307–14. doi: 10.1016/j.jcis.2020.06.077
42. Cui Y, Duan W, Jin Y, Wo F, Xi F, Wu J. Ratiometric fluorescent nanohybrid for noninvasive and visual monitoring of sweat glucose. *ACS Sens.* (2020) 5:2096–105. doi: 10.1021/acssensors.0c00718
43. Zhang L, Li S, Sun Y, Xiao K, Song G, Lu P, et al. Self-assembly of flavin mononucleotide and a cationic polythiophene in aqueous media: spectroscopic studies and sensing applications. *Polym Chem.* (2020) 11:3762–7. doi: 10.1039/D0PY00403K
44. Hu Y, Zhuang X, Lin L, Liu J, Yao Z, Xiao Z, et al. Determination of Ag(I) and NADH using single-molecule conductance ratiometric probes. *ACS Sens.* (2020) 6:461–9. doi: 10.1021/acssensors.0c02038
45. Zhang L, Zhao Y, Wu Y, Jiang Y, Wang Q, Lin X, et al. An efficient approach for rapid detection of polymyxins B based on the optically active supramolecular aggregates of water-soluble perylene diimide. *Sens Actuators, B.* (2020) 321:128594–600. doi: 10.1016/j.snb.2020.128594
46. Zhang L, Sun Y, Jiang Y, Li Y, Song G, Huang K, et al. Visual sensing of picric acid in 100% aqueous media based on supramolecular polythiophene assemblies with colorimetric and fluorescent dual response. *Chin Chem Lett.* (2020) 31:2428–32. doi: 10.1016/j.ccl.2020.04.003
47. Szentirmay MN, Martin CR. Ion-exchange selectivity of nafion films on electrode surfaces. *Anal Chem.* (2002) 56:1898–902. doi: 10.1021/ac00275a031
48. Ma K, Zheng Y, An L, Liu J. Ultrasensitive immunosensor for prostate-specific antigen based on enhanced electrochemiluminescence by vertically ordered mesoporous silica-nanochannel film. *Front Chem.* (2022) 10:851178. doi: 10.3389/fchem.2022.851178
49. Basnig D, Vilá N, Herzog G, Walcarius A. Voltammetric behaviour of cationic redox probes at mesoporous silica film electrodes. *J Electroanal Chem.* (2020) 872:113993–9. doi: 10.1016/j.jelechem.2020.113993
50. Gong J, Zhang T, Chen P, Yan F, Liu J. Bipolar silica nanochannel array for dual-mode electrochemiluminescence and electrochemical immunosensing platform. *Sens Actuators, B.* (2022) 368:132086–93. doi: 10.1016/j.snb.2022.132086
51. Xiao Y, Chen S, Zhang S, Wang G, Yi H, Xin G-Z, et al. Mesoporous silica-mediated controllable electrochemiluminescence quenching for immunosensor with simplicity, sensitivity and tunable detection range. *Talanta.* (2021) 231:122399–406. doi: 10.1016/j.talanta.2021.122399
52. Ko K, Park S, Lim H, Park S, Kim M. Improved pretreatment method for determination of nisin a and z and monitoring in cheese using liquid chromatography-tandem mass spectrometry. *Food Anal Methods.* (2015) 9:122–30. doi: 10.1007/s12161-015-0158-y
53. Rossano R, Del Fiore A, D'Elia A, Pesole G, Parente E, Riccio P. New procedure for the determination of nisin in milk. *Biotechnol Tech.* (1998) 12:783–6. doi: 10.1023/A:1008820803070
54. Soliman LC, Donkor KK. Method development for sensitive determination of nisin in food products by micellar electrokinetic chromatography. *Food Chem.* (2010) 119:801–5. doi: 10.1016/j.foodchem.2009.06.062